

Lead-Free Perovskite Nanostructures: A Step Toward Sustainable High-Efficiency Solar Cells

Kawther A. Khalaph¹, Nisreen Kh. Abdalameer², Abdallah Ben Rhaïem³, Aqel Mashot Jafar⁴

¹Medical College, IbnSina University of Medical and Pharmaceutical Sciences, Baghdad, Iraq.

²Department of Physics, College of Science for Women, University of Baghdad, Iraq.

³Department of Physics, Faculty of Sciences, University of Sfax, BP 1171 Sfax 3000, Tunisia

⁴Research and Technology Center of Environment, Water, and Renewable Energy, Scientific Research Commission, Ministry of Higher Education and Scientific Research, Baghdad, Iraq.

Article Info

Article history:

Received: 17, 11, 2025

Revised: 30, 12, 2025

Accepted: 23, 01, 2026

Published: 30, 03, 2026

Keywords:

lead-free dual perovskite,
band gap,
solar cells,
power conversion efficiency.

ABSTRACT

Dual perovskite materials that are lead-free remain of great interest to the research community due to their potential utility in photocatalysis and electronics, and, without lead, they can be used as non-environmentally toxic materials. In light of the global trend towards replacing lead-containing materials with safer alternatives, this study focuses on employing $ZnSnO_3$ as a lead-free option to reduce the environmental and health risks associated with conventional photovoltaic materials while maintaining electronic and optical properties suitable for solar applications. This work developed a low-cost, environmentally friendly method to produce $ZnSnO_3$ composites and to test their effectiveness as an active layer in solar cells. The device consists of an FTO/TiO₂/ZnSnO₃/CuO/Al stack structure. The $ZnSnO_3$ film is very crucial due to its ability to harvest visible light and accelerate the charge transfer. The samples were examined by X-ray diffraction (XRD), ultraviolet-visible (UV-Vis) spectroscopy and field emission scanning electron microscopy (FESEM). This indicated that the nanoparticles have a uniform morphology and unique optical properties. Measurements indicated that the $ZnSnO_3$ has a direct band gap of around 3.32 eV. This makes it able to absorb a lot of sunlight. At an illumination of under 100 mW/cm², the cell prepared with this structure also showed a power conversion efficiency of 5.6%. Such results indicate that room temperature $ZnSnO_3$ is a possible attractive medium to enhance environmentally friendly solar cells

This is an open-access article under the CC BY license.



Corresponding Author:

Abdallah Ben Rhaïem

Department of Physics, Faculty of Sciences,
University of Sfax, BP 1171 Sfax 3000 Tunisia

Email: abdallah.benrhaïem@fss.usf.tn



1. INTRODUCTION

There are two primary configurations of planar-structured perovskite solar cells (PSCs): n-i-p and p-i-n. A perovskite active layer is inserted between an electron transport layer (ETL) and a hole transport layer (HTL) in these cells[1]. Perovskite materials are becoming increasingly popular as semiconductors, largely because they have a high absorption coefficient for light (which is good for use in solar cells). Nanomaterials have been the subject of much recent interest due not only to their potential to improve device performance, but also the distinct physical and chemical properties with which they set themselves apart from bulk materials[2]. The efficiency with which perovskite solar cells turn power into electricity has also skyrocketed, from just 3.8% to 25.5%[3]. That it is among the best of new technologies for turning out cheap solar cells. Some semiconductors, like CuO[4], $ZnSnO_3$ and TiO₂ environmental safe materials. They draw a lot of curiosity, because they have rich photoconductivity and show high photochemical performance. These materials are characterised by high optical conductivity and active photochemical activity, making them useful for a variety of applications, including photovoltaic energy conversion devices and gas sensors[5][6] [7]. In this instance, a metal-oxide-based active electrode is employed in PSCs (metals such as TiO₂, $ZnSnO_3$ or CuO that are deposited as thin films on fluorine-doped tin oxide (FTO) glass).

The ZTO composite can perform better than the pure oxides in the aspects of thermal stability, electrical conductivity and response in the visible-ultraviolet range. Some studies have shown that ZnSnO₃ has a wide energy gap and optical properties suitable for photovoltaic applications, as its nanoparticles were prepared by the sol-gel method while studying its structural and optical properties [8]. Other studies have shown that thin films of ZnSnO₃ have high transparency, exceeding 85% in the visible range, with an energy gap of approximately 3.3 electron volts, which enhances their potential use in optical devices and solar cells [9]. Several researchers have also pointed out that ZnSnO₃ is a perovskite oxide with a wide energy gap, ranging from 3.5 to 3.6 electron volts depending on the preparation method, which makes it suitable for energy conversion and photovoltaic applications [10]. The present work aims to explore the feasibility of using lead-free double-structured perovskite (ZnSnO₃) as an active layer for solar cells, which is fabricated as a thin film by a simple and environmentally friendly solution process, and to propose an innovative solar cell architecture based on FTO/ TiO₂/ ZnSnO₃/CuO/Al. The research serves as a normative data model to systematically correlate the structure and optical properties of ZnSnO₃ with its application performance, guiding this solar cell innovation toward sustainable energy production.

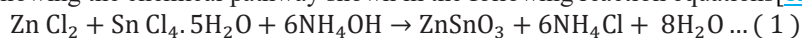
2. Experimental Methodology

2.1 Materials.

A conductive FTO glass substrate with a surface resistivity of 15 Ω was used in this study, and distilled deionized water was used as the solvent. We have also employed hydrated tin chloride (SnCl₄ · 2H₂O, 99% purity, Sigma Aldrich), zinc chloride (ZnCl₂, 99.9% purity, BHD) and ammonium hydroxide (NH₄OH, 99.9% purity, FlukaChemika), as well as aluminum wire (Al, 99.9% pure) for the synthesis of the studied objects.

2.2 Preparation of Lead-Free Double Perovskite (LFDPVS)

Zinc stannate perovskite solutions and thin films are prepared by various methods. Most previous studies have indicated that the formation of ZnSnO₃ nanoparticles typically occurs via the reduction reaction of a mixture of zinc and tin salts dissolved in aqueous medium, in the presence of ammonium hydroxide, under hydrothermal conditions [11]. In this work, a similar approach was adopted to prepare ZnSnO₃ (Chemical precipitation), following the chemical pathway shown in the following reaction equations [12].



10 g of hydrated tin chloride (SnCl₄ · 5H₂O) was dissolved in 50 ml of distilled, deionised water in a glass flask, which was placed on a hot plate at a constant temperature of 70 °C and stirred continuously for 30 min. Similarly, 3.887 g of zinc chloride (ZnCl₂) was dissolved in 50 ml of distilled deionised water in another flask under similar heating and stirring conditions. After obtaining two homogeneous solutions of zinc and tin salts, they were combined with continuous stirring for 30 min, followed by the addition of 6.18 ml of ammonium hydroxide (NH₄OH) solution to the mixture. The mixture was then heated with continuous stirring for 60 min, resulting in the precipitation of a yellowish-white solid, representing the initial phase of the intermediate compound ZnSnO₃.



Figure (1): Form of the prepared material (ZnSnO₃)

2.3 PV Device Fabrication

The initial (TiO₂) solution was deposited onto a transparent, conductive glass (FTO) substrate using a drop-casting method at 70 °C, yielding a substrate surface resistivity of 15 Ω. A perovskite (ZnSnO₃) solution was then deposited onto the preheated FTO/ TiO₂ substrates at the same temperature (70 °C) using the same technique. Copper oxide (CuO) was then deposited onto the FTO/ TiO₂/ ZnSnO₃ substrates to obtain the final FTO/ TiO₂/ ZnSnO₃/CuO samples. A 0.1 cm² aluminium foil was then placed on top of the CuO layer as an electrode, as shown in Figure 2, which illustrates the thin-film structure of the photovoltaic (PV) device.

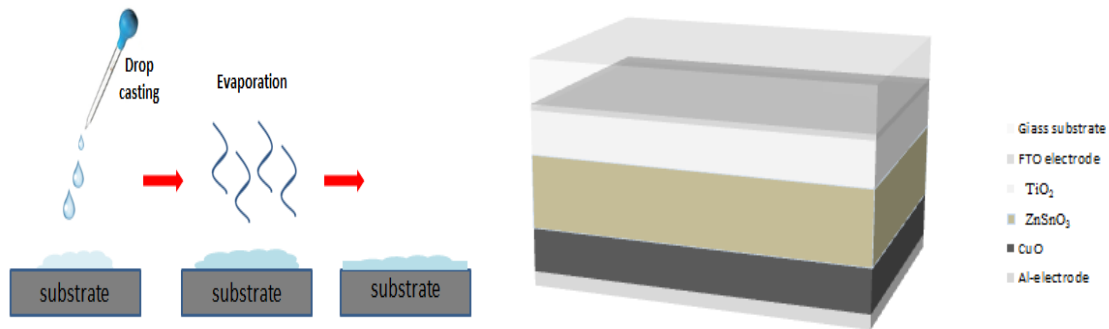


Figure (2): Diagram of Photo-Voltaic showing (FTO/ TiO₂/ ZnSnO₃/CuO/Al) layer deposited on FTO.

2.4 A characterisation of the sample

The structure of the thin films was studied using a Shimadzu 6000 equipped with Cu-K α radiation, using X-ray diffraction (XRD). The average crystallite size (D), which can be estimated using Scherrer's formula:

$$D = \frac{K\lambda}{\beta \cos\theta} \dots \dots (2)$$

Where (D) is the Crystallite size, (K) is the shape factor (taken as 0.94), (λ) is the wavelength (1.5406 Å) of the X-ray, and (β) is the full peak width at half maximum (FWHM). To analyse the morphology of the crystalline films, the samples were examined using a scanning electron microscope (SEM), manufactured by Bruker Nano GmbH in Germany. Absorption and transmittance measurements were also performed using a UV/Vis Double Beam (UVD-3500) spectrometer. From the absorption peak, the energy band gap was calculated using the Tauc relation:

$$(\alpha h\nu) = B (h\nu - E_g)^n \dots \dots (3)$$

Where (α) is the absorbance coefficient, (h) is Planck's constant, (B) is the empirical constant, (ν) is the light frequency, E_g is the energy band gap, (n) is a constant, which depends on the transmission either (1/2) for direct (allowed). The current-voltage (I-V) characteristics of the LFPVSC device were studied using a Keithley 2400 source/measurement meter, under simulated standard illumination conditions of AM 1.5 G with a light intensity of $10^2 \text{ W} \cdot \text{m}^{-2}$. The PCE of a solar cell may be determined with the use of equation (4) [13]

$$PCE = \frac{J_m V_m}{P_{in}} = \frac{V_{oc} \cdot I_{sc} \cdot FF}{P_{in} \cdot A_{sc}} * 100\% \dots \dots (4)$$

Where, F.F: Fill Factor, V_m : Maximum Voltage, J_m : Maximum current density, I_m : The maximum value of the current, A: Area of the solar cell, and P_m : maximum power.

3. RESULTS AND DISCUSSION

3.1. XRD analysis

X-ray diffraction (XRD) was used to determine the crystal structure, crystallite size, and phase of the fabricated thin film.

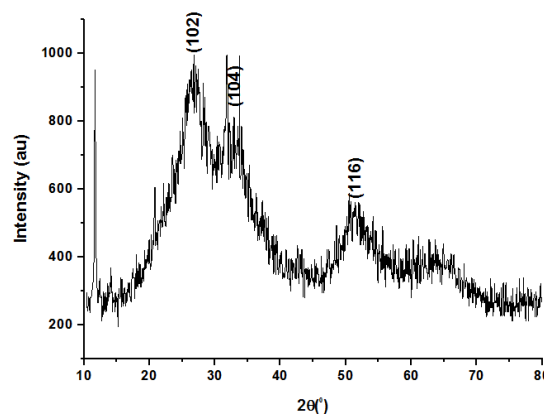


Figure 3: XRD pattern of ZnSnO₃ thin film

Figure 3 shows the XRD patterns of a ZnSnO_3 thin film deposited on a glass substrate by the drop-coating method. Specific peaks were observed at 2θ angles of 26.67° , 32.89° , and 51.45° , corresponding to the tetragonal phase planes (102), (104), and (116), respectively. The detected XRD pattern closely matches the data in JCPDS card No. 28-1486. As there are no other peaks, the material is therefore determined as pure in crystalline nature. We also observe that the widening of the diffraction peaks is likely related to the small crystal size and the presence of lattice stress, which is commonly associated with nanomaterials. It should also be noted that some of the peak widening may be due to the instrument's response during measurement. As high charge mobility is pretty essential for high-quality solar cells, the perovskite films with well-packed crystalline sections show an enhanced charge transfer. This leads to the possibility of improving the performance of optoelectronic devices by increasing the crystallinity of the perovskite layer and orienting its crystals. The crystal size was determined using the Debye–Scherrer equation, yielding an average crystal size of ≈ 33 nm.

Table 1: Structural parameters of ZnSnO_3

| Prepared methods | 2θ (deg) | FWHM (deg) | d-spacing observed(\AA) | (hkl) | crystal size (nm) |
|-------------------------------|-----------------|------------|------------------------------------|-------|-------------------|
| JCPDS No. 28-1486 | 26.67 | 1.8980 | 3.42 | (102) | 41.5 |
| | 32.89 | 2.4516 | 2.81 | (104) | 35.1 |
| | 51.45 | 3.8960 | 1.81 | (116) | 22.4 |
| Average Crystallite size (nm) | | | | | 33.3 |

3.2. FE-SEM analysis

The surface morphology of an LFDPVs thin film deposited on a glass substrate was examined using field-emission scanning electron microscopy (FESEM). **Figure 4** shows micrographs of a nanostructured polycrystalline film, with spherical and non-spherical grains observed across the entire surface in different sizes. Such structural distribution shows formation of perovskite grains in large size, which are crucial for efficient charge transportation and low carrier recombination, implying this structure is favorable for high-performance solar cells. Clusters of growing nanoparticles on the surface are also observed in the image, and uniformly distributed micropores and microbridges enhance the effective surface area and promote interlayer contact in a photovoltaic device.

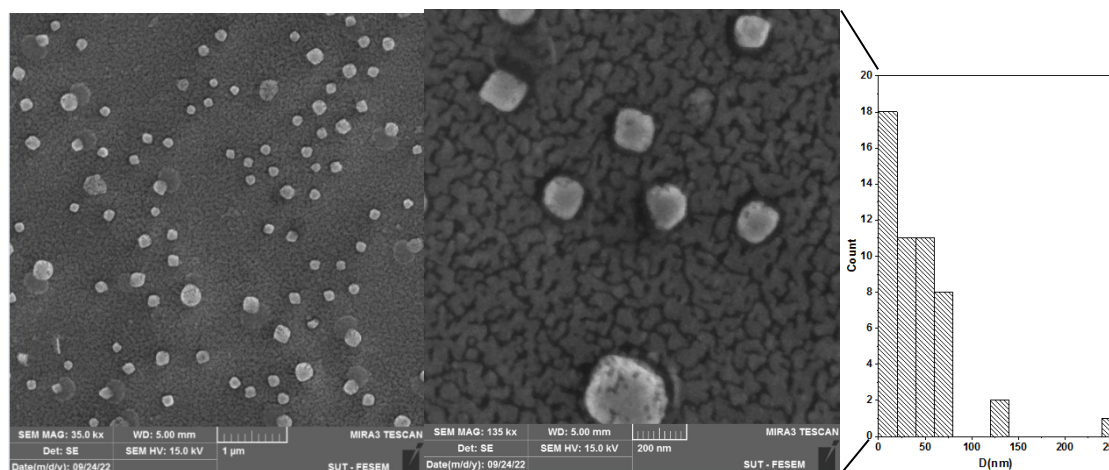


Figure 4: FE-SEM image of ZnSnO_3 thin film

3.3. Optical Properties

The photovoltaic response of the ZnSnO_3 film was examined for optical absorption, **Figure 5**, after deposition on the glass substrate using a UV-Vis spectrometer. The spectra exhibited high transparency in the visible range (100–1200 nm), indicating that this film is promising as a solar cell window layer. In contrast, strong absorption was observed in the UV range (300–400 nm), with a sharp absorption edge at about 337 nm.

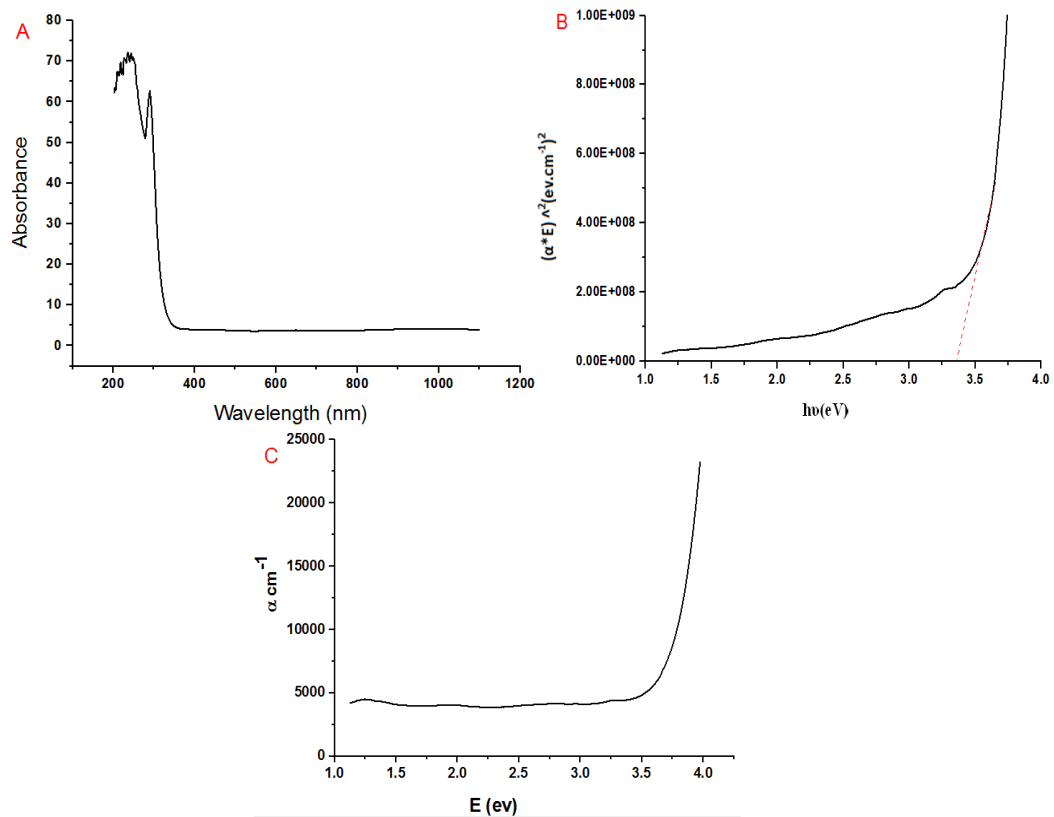


Figure 5: a. optical absorbance, b. calculating the energy gap using the Tauc equation of the ZnSnO₃ double perovskite film. c. The absorption coefficient changes with the photon's energy.

Figure 5a shows the absorption spectrum, indicating that the material exhibits high absorption in the ultraviolet region, while absorption gradually decreases in the visible region. This behavior is attributed to electron transitions from the valence band to the conduction band, resulting in a distinct absorption edge at specific wavelengths related to the material's energy gap. Figure 5b shows the determination of the optical energy gap. Tauc's equation, suitable for direct-transition semiconductors, was used to plot the relationship between $(\alpha \cdot E)^2$ and the photon energy. The linear portion of the curve is clearly visible at higher energies, and by extending this portion to its intersection with the energy axis, the optical energy gap was estimated to be approximately 3.3 eV. This value indicates that the material possesses a relatively wide energy gap, consistent with the nature of semiconducting oxides. Figure 5c shows that the absorption coefficient (α) was calculated from the absorbance data and then plotted as a function of photon energy. The results showed that the absorption coefficient increases with increasing photon energy and becomes more pronounced near the absorption edge, indicating the presence of strong electronic transitions in this spectral region. This optical behavior can also be attributed to the material's nanostructure, as the small crystal size can influence the nature of electronic transitions and enhance the material's interaction with light. Taken together, these results indicate that the material possesses optical properties suitable for use in optoelectronic applications.

3.4. (I-V) Properties to solar cell

Measuring the current-voltage curve under illumination is one of the most important electrical tests for solar cells. It is used to evaluate the cell's operational characteristics and extract its key parameters that determine its efficiency. Figure (6) shows the current curves under a forward bias voltage under standard illumination conditions (100 mW/cm²). It is observed that the photocurrent increases exponentially with applied voltage under forward bias, due to the increased charge-carrier injection rate at higher voltages. The open-circuit voltage (V_{oc}) [14] was determined from the point of intersection of the curve with the x-axis at ($I = 0$), while the short-circuit current (I_{sc}) was obtained from the point of intersection of the curve with the y-axis at ($V = 0$). The maximum power output from the solar cell is calculated from the product of the open-circuit voltage and the short-circuit current ($P_{out} = V_{oc} \times I_{sc}$).

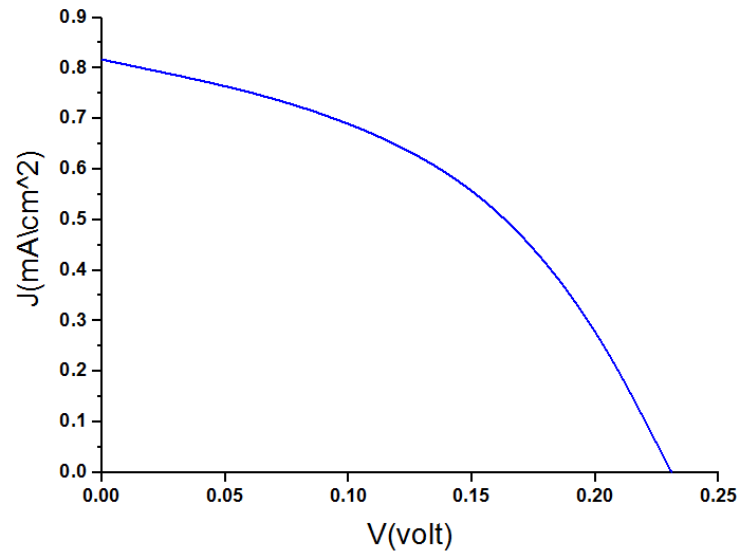


Figure 6: Performance of (FTO/ TiO₂/ ZnSnO₃/CuO/Al) solar cell.

Table (2) : also provides detailed values for the measured solar cell parameters.

| solar cells (Configurations) | V _{oc} (V) | J _{sc} (mA/cm ²) | V _m (V) | J _m (mA/cm ²) | F.F | PCE% |
|---|------------------------|--|-----------------------|---|-----|------|
| FTSA t _{TiO₂} ≈ 175.1 nm, and t _{ZnSnO₃} ≈ 150.2 nm and t _{CuO} = 151.2 nm. R _s =3.3 kΩ R _{sh} =4.62kΩ | 0.6 | 12.2 | 0.46 | 12.1 | 76 | 5.6 |

Based on these values, the photoconversion efficiency (η) was calculated using Equation (2) for all studied samples. The highest efficiency ($\eta = 5.6\%$) was achieved for the layered structure composed of: (FTO/TiO₂/ZnSnO₃/CuO/Al). This performance can be explained by improved charge-carrier separation and transport within the device, resulting from the alignment of the energy levels of the transport layers and the active layer. The TiO₂ layer acts as an electron-transport layer, while the CuO layer contributes to hole transport, thereby reducing charge-carrier recombination at the interfaces. Furthermore, the presence of the ZnSnO₃ nanolayer provides a large surface area and good optical properties, thereby enhancing light absorption and facilitating charge transport. This is reflected in an increased current density (J_{sc}) and an improved fill factor (FF), resulting in a higher photoconversion efficiency for the prepared solar cell.

4. CONCLUSION

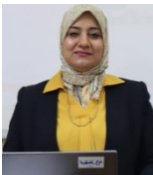





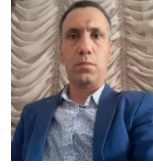





In the present work, the prepared material was fabricated and investigated for its structural, optical, and electrical characteristics. The measurements demonstrated the success of the preparation and basic properties for photovoltaic applications. The characteristic J–V (current density–voltage) curves for the solar cell we prepared demonstrated a short-circuit current density value of (12.2 mA/cm²) and open-circuit voltage of (0.6V). The fill factor (76%) and photoconversion efficiency (5.6%) are typical, suggesting there is still room for improvement. Thus, the study concludes that the synthesised material could be used in solar cells. But the increased efficiency requires higher-quality structures and fewer surface and interfacial defects for practical performance.

REFERENCES

- [1] K. A. Khalaph and A. M. Jafar, "Lead-free Two-dimensional Perovskite Solar Cells Cs₃Fe₂Cl₉ Using MgO Nanoparticulate Films as Hole Transport Material," *NeuroQuantology*, vol. 18, no. 2, pp. 127–132, 2020. 10.14704/nq.2020.18.2.NQ20137.
- [2] P. Granitzer, K. Rumpf, T. Ohta, N. Koshida, P. Poelt, and M. Reissner, "Porous silicon/Ni composites of high coercivity due to magnetic field-assisted etching," *Nanoscale Res. Lett.*, vol. 7, no. 1, p. 384, Dec. 2012. 10.1186/1556-276X-7-384
- [3] H. Zhang, X. Ji, H. Yao, Q. Fan, B. Yu, and J. Li, "Review on efficiency improvement effort of perovskite solar cell," *Sol. Energy*, vol. 233, pp. 421–434, Feb. 2022. DOI:10.1016/j.solener.2022.01.060
- [4] Z.-K. Yu et al., "Solution-processed CuO as an efficient hole-extraction layer for inverted planar heterojunction perovskite solar cells," *Chinese Chem. Lett.*, vol. 28, no. 1, pp. 13–18, Jan. 2017. <https://doi.org/10.1016/j.ccl.2016.06.021>
- [5] K. A. Khalaph, Z. J. Shanan, F. Mustafa Al-Attar, A. N. Abd, and A. Mashot Jafar, "Fabrication and investigation of hybrid Perovskite solar cells based on porous silicon," *Mater. Today Proc.*, vol. 20, no. 3, pp. 605–610, 2020. DOI: 10.1016/j.matpr.2019.09.197

- [6] S. M. A. Z. Shawon et al., "Surface modified hybrid ZnSnO₃ nanocubes for enhanced piezoelectric power generation and wireless sensory application," *Nano Energy*, vol. 92, p. 106653, Feb. 2022. DOI:10.1016/j.nanoen.2021.106653
- [7] M. Basante-Romo, J. O. Gutiérrez-M, and R. Camargo-Amado, "Non-toxic doses of modified titanium dioxide nanoparticles (m-TiO₂NPs) in albino CFW mice," *Heliyon*, vol. 7, no. 3, p. e06514, Mar. 2021. DOI: 10.1016/j.heliyon.2021.e06514.
- [8] D. M. Ibrahim, A. A. Gaber, A. E. Reda, D. A. Abdel Aziz, and N. A. Ajiba, "Structural, optical, and dielectric properties of sol-gel derived perovskite ZnSnO₃ nanomaterials," *J. Sol-Gel Sci. Technol.*, vol. 112, no. 3, pp. 703–714, Dec. 2024. DOI: 10.1007/s10971-024-06550-2.
- [9] M. Rajesh and B. Rajalingam, "A modified sol-gel synthesis protocol for high-quality ZnSnO₃ thin films with enhanced electrical and optical properties for energy and sensor applications," *MethodsX*, vol. 15, p. 103629, Dec. 2025. DOI: 10.1016/j.mex.2025.103629.
- [10] R. Indhumathi, A. S. Priya, and B. S. Samyuktha, "Analyzing the Thermal Behavior and Phase Transitions of ZnSnO₃ Prepared via Chemical Precipitation †," *Eng. Proc.*, vol. 87, no. 1, 2025. DOI: 10.3390/engproc2025087004.
- [11] D. Mukherjee, M. Hordagoda, C. Kons, A. Datta, S. Witanachchi, and P. Mukherjee, "Measurements of Polarization Switching in LiNbO₃ -type ZnSnO₃ /ZnO Nanocomposite Thin Films," *MRS Proc.*, vol. 1729, pp. 111–116, Mar. 2015. DOI: 10.1557/opl.2015.264.
- [12] N. K. Abdalameer, K. A. Khalaph, and A. M. Jafar, "Synthesis of ZnO, SnO₂, (ZnSnO₃) perovskite structure by chemical method and evaluation of antimicrobial activity," *Eur. Phys. J. Plus*, vol. 140, no. 4, p. 294, Apr. 2025. DOI: 10.1140/epjp/s13360-025-06233-z.
- [13] K. A. Khalaph, Z. J. Shanan, A. M. Jafar, and F. M. Al-Attar, "Double Nanoperovskite Heterojunctions Based on SI-Porous," *Int. J. Nanosci.*, vol. 22, no. 03, pp. 1–7, Jun. 2023.
- [14] H. Maheshkant et al., "Materials Science & Engineering B Open-circuit voltage (V_{oc}) enhancement through integration of MoS₂ layer at the interface between Mo and Sb₂S₃," *Mater. Sci. Eng. B*, vol. 321, no. June, 2025.

BIOGRAPHIES OF AUTHORS

| | |
|---|--|
|  | <p>Kawther A. Khalaphis is an Assistant Professor at the Medical College, Ibn Sina University of Medical and Pharmaceutical Sciences, Baghdad University, Iraq. She received the B.Sc. degree in Physics from Ibn Al-Haytham College of Education for Pure Sciences. the University of Baghdad, and the M.Sc. degree in Physics from Baghdad University, Iraq. She holds a PhD degree in physics. Her research areas are nanotechnology, nanomedicine, and medical physics. She has published several scientific papers in national and international conferences and journals. She can be contacted at email: kawther.ali@ibnsina.edu.iq</p> |
| | <p>Scopus®  </p> |
|  | <p>Nisreen Kh. Abdalameera is an Assistant Professor at the College of Science for Women, Baghdad University, Iraq. She received the B.Sc. degree in Physics from the University of Baghdad and the M.Sc. degree in plasma physics from the University of Baghdad, Iraq. She holds a PhD degree in physics. Her research areas are plasma, plasma medicine, and nanotechnology. She has published several scientific papers in national and international conferences and journals. She can be contacted at email: nisreenka_phys@csw.uobaghdad.edu.iq</p> |
| | <p>Scopus®  </p> |
|  | <p>Abdallah Ben Rhaïem: Professor of Physics at the Faculty of Sciences of Sfax and Director of the LaScOM laboratory. His current research focuses on the structural, morphological, optical, dielectric, electrical, and electrochemical analyses of various systems used as positive electrode materials for sodium-ion batteries and as halide perovskites for optoelectronic applications. He can be contacted at email: abdallah.benrhaïem@fss.usf.tn</p> |
| | <p>Scopus®  </p> |
|  | <p>Aqel Mashot Jafar is a senior research scientist at the Centre for Environmental, Water, and Renewable Energy Research and Technology, Scientific Research Authority, Ministry of Higher Education and Scientific Research, Iraq. He received his Bachelor of Science degree in Physics from the College of Science at Al-Mustansiriya University and his Master of Science degree in Physics from the University of Baghdad, Iraq. He holds a PhD in Physics from the College of Science at the University of Baghdad. His research interests in renewable energy include solar cell applications and the preparation and study of perovskite solar cells. He has published numerous scientific papers in local and international conferences and journals. He can be contacted via email: aqel.m.jafar@src.edu.iq</p> |
| | <p>Scopus®  </p> |